Electronic Supplementary Information (ESI)

For

Insight into the effects of calcination temperature on the structure-performance of RuO_2/TiO_2 in the Deacon process

Siyao Li,[a] Bowen Xu,[a] Yuexia Wang,[a] Yupei Liu,[a] Xinqing Lu,*[a,b] Rui Ma,[a,b] Yanghe Fu,[a,b] Shuhua Wang,[c] Liyang Zhou[c] and Weidong Zhu*[a,b,c]

[a] *Zhejiang Engineering Laboratory for Green Syntheses and Applications of Fluorine-Containing Specialty Chemicals, Institute of Advanced Fluorine-Containing Materials, Zhejiang Normal University, 321004 Jinhua, People's Republic of China*

[b] *Key Laboratory of the Ministry of Education for Advanced Catalysis Materials, Institute of Physical Chemistry, Zhejiang Normal University, 321004 Jinhua, People's Republic of China*

[c] *National Engineering Technology Research Center of Fluoro-Materials, Zhejiang Juhua Technology Center Co., Ltd., 324004 Quzhou, People's Republic of China*

*To whom correspondence should be addressed.

Tel./Fax: +86 579 82282234; E-mail: xinqinglu@zjnu.cn (X. Lu);

Tel./Fax: +86 579 82282932; E-mail: weidongzhu@zjnu.cn (W. Zhu)

Mass Transfer Calculation for HCl Oxidation over RuO_2/TiO_2

The effects of internal and external transfer limitations on reaction kinetics were evaluated by the Mears (C_M) and Weisz-Prater (C_{WP}) criteria, respectively,[1,2] which were calculated using the following formulas:

$$C_M=\frac{nr_{obs}\rho_{catal.}R_{catal.}}{k_cC_{HCl}} \quad (S1)$$

$$C_{WP}=\frac{r_{obs}\rho_{catal.}R_{catal.}^2}{D_{eff}C_{HCl,s}} \quad (S2)$$

where n is the reaction order, r_{obs} is the observed reaction rate, $\rho_{catal.}$ is the bulk density of catalyst bed, $R_{catal.}$ is the particle radius of catalyst, k_c and D_{eff} are the external mass transfer coefficient and effective diffusion coefficient, respectively, C_{HCl} and $C_{HCl,s}$ are the bulk concentration of HCl and the HCl concentration on the surface of a catalyst particle, respectively. $C_{HCl,s}$ is equal to C_{HCl} when the external transfer limitation is excluded.

k_c was estimated by the combination of Sherwood number Sh, the Reynolds number Re_p, and the Schmidt number Sc using the following formulas:

$$Sh=\frac{k_cd_{catal.}}{D_{eff}}=2+0.6Re_p^{1/2}Sc^{1/3} \quad (S3)$$

$$Re_p=\frac{U\rho d_{catal.}}{\mu} \quad (S4)$$

$$Sc=\frac{\mu}{D_{eff}\rho} \quad (S5)$$

Where $d_{catal.}$ is the catalyst particle size, U is the free-stream velocity, ρ and μ are the density and viscosity of a feed mixture, which can be obtained from Aspen Plus software.

D_{eff} was estimated by the combination of the coefficients for Knudsen diffusion D_A^K and bulk diffusion D_A^b using the following formulas:

$$\frac{1}{D_{\text{eff}}}=\frac{1}{D_{\text{A}}^{\text{K}}}+\frac{1}{D_{\text{A}}^{\text{b}}} \tag{S6}$$

$$D_{\text{A}}^{\text{K}}=\frac{2}{3}r_{\text{po}}\sqrt{\frac{8\text{RT}}{\pi M_{\text{i}}}}\frac{\varepsilon}{\tau} \tag{S7}$$

$$r_{\text{po}}=4\frac{\varepsilon}{S_{\text{catal.}}\rho_{\text{catal.,g}}} \tag{S8}$$

$$D_{\text{A}}^{\text{b}}=D_{\text{A}}\frac{\varepsilon}{\tau} \tag{S9}$$

where r_{po}, ε, τ, $S_{\text{catal.}}$, and $\rho_{\text{catal.,g}}$ are the average pore radius, porosity, tortuosity, surface areas, and grain density of catalyst, respectively, T and M_{i} are the temperature and relative molecular weight of component i, respectively, and D_{A} is the free diffusion coefficient, which can be obtained from Aspen Plus software.

The data used in the above-mentioned equations and the calculations of the Mears and Weisz-Prater parameters are shown in Tables S2 and S3. Both external and internal mass transfer limitations can be excluded for all the kinetic study cases, as C_{M} and C_{WP} are less than 0.15 and 1, respectively.

References

1. H.S. Fogler, Diffusion and reaction in Elements of Chemical Reaction Engineering; Pearson Education Inc.: New York, 2016, pp 734-743.

2. T.R. Marrero, E.A. Mason, Gaseous diffusion coefficients, Journal of Physical and Chemical Reference Data, 1972, 1, 1-118.

Table S1 Physicochemical properties of TiO_2 and RuO_2/TiO_2 catalysts

Table S2 Measured reaction rates over RuO_2/TiO_2 catalysts at different reaction temperatures for E_a calculations

Table S3 Data for calculating the Mears and Weisz-Prater criterion parameters

Table S4 Evaluation of the Mears (C_M) and Weisz-Prater (C_{WP}) criterion parameters

Fig. S1 Wide-angle XRD patterns of RuO_2/TiO_2-150 (a), RuO_2/TiO_2-200 (b), RuO_2/TiO_2-250 (c), RuO_2/TiO_2-300 (d), and RuO_2/TiO_2-350 (e). The standard pattern of rutile-type TiO_2 (JCPDS No. 21-1276) is shown at the bottom of the figure.

Fig. S2 SEM image of TiO_2.

Fig. S3 Ru 3d XPS spectrum of $RuCl_3/TiO_2$.

Fig. S4 Cl 2p XPS spectra of $RuCl_3/TiO_2$ (A), RuO_2/TiO_2-150 (B), RuO_2/TiO_2-200 (C), RuO_2/TiO_2-250 (D), RuO_2/TiO_2-300 €, and RuO_2/TiO_2-350 (F).

Fig. S5 EDX mapping images of Cl for $RuCl_3/TiO_2$ (A), RuO_2/TiO_2-150 (B), RuO_2/TiO_2-200 (C), RuO_2/TiO_2-250 (D), RuO_2/TiO_2-300 (E), and RuO_2/TiO_2-350 (F).

Fig. S6 TEM (A, E) and EDX mapping images of Ru (B, F), O (C, G), and Ti (D, H) for RuO_2/TiO_2-250 (A-D) and RuO_2/TiO_2-350 (E-H).

Fig. S7 Effects of HCl flow rate and reaction temperature on the catalytic activities in the oxidation of HCl with O_2 over different RuO_2/TiO_2 catalysts. Reaction conditions: catalyst particle sizes = 0.180-0.250 mm, WHSV (HCl) = 2933 h^{-1}, and molar ratio of HCl to O_2 = 4 : 1.

Fig. S8 Effects of catalyst particle size and reaction temperature on the catalytic activities in the oxidation of HCl with O_2 over different RuO_2/TiO_2 catalysts. Reaction

conditions: WHSV (HCl) = 2933 h^{-1} and molar ratio of HCl to O_2 = 4 : 1.

Fig. S9 Heat flow and MS signals in the microcalorimetric measurements on the pulse adsorption of O_2 on RuO_2/TiO_2-250 (A, B) and RuO_2/TiO_2-350 (C, D), respectively, as a function of time at 350 ºC.

Fig. S10 Raman spectra of the fresh RuO_2/TiO_2-350 (a) and the used RuO_2/TiO_2-350 (b). The used catalyst represents the catalyst after 32 h of the reaction at 350 °C, and the reaction conditions were the same as those described in the caption of Fig. 4.

Fig. S11 Effects of WHSV on the oxidation of HCl over RuO_2/TiO_2-250. Reaction conditions: molar ratio of HCl to O_2 = 1 : 1 and reaction temperature = 350 °C.

Table S1 Physicochemical properties of TiO_2 and RuO_2/TiO_2 catalysts

Samples	Ru loading[a] (wt.%)	S_{BET}[b] ($m^2\ g^{-1}$)	S_{ext}[c] ($m^2\ g^{-1}$)	V_{micro}[c] ($cm^3\ g^{-1}$)	V_{total}[d] ($cm^3\ g^{-1}$)
TiO_2	-	34.8	34.7	0.0	0.25
RuO_2/TiO_2-150	2.1	35.8	34.7	0.0	0.25
RuO_2/TiO_2-200	2.0	36.3	35.0	0.0	0.26
RuO_2/TiO_2-250	2.0	36.8	34.5	0.0	0.27
RuO_2/TiO_2-300	1.9	34.9	33.8	0.0	0.27
RuO_2/TiO_2-350	2.0	35.4	35.0	0.0	0.26

[a] Determined from ICP-AES analysis.

[b] Determined from the measured N_2 adsorption-desorption isotherms at -196 °C using the Brunauer-Emmett-Teller (BET) method.

[c] Determined from the measured N_2 adsorption-desorption isotherms at -196 °C using the *t*-plot method.

[d] Determined from the N_2 adsorption isotherm at -196 °C using the single-point method at a relative pressure of 0.995.

Table S2 Measured reaction rates over RuO_2/TiO_2 catalysts at different reaction temperatures for E_a calculations[a]

Catalyst	Temperature (°C)	HCl conversion (%)	Reaction rate ($\times 10^{-4}$ mol g^{-1} s^{-1})
RuO_2/TiO_2-150	330	2.7	6.03
	335	3.2	7.15
	340	3.8	8.48
	345	4.5	10.04
	350	5.2	11.61
	355	6.1	13.62
	360	7.3	16.29
RuO_2/TiO_2-200	330	3.3	7.37
	335	3.9	8.63
	340	4.5	10.04
	345	5.3	11.83
	350	6.1	13.62
	355	7.1	15.85
	360	8.2	18.30
RuO_2/TiO_2-250	330	4.0	8.97
	335	4.6	10.34
	340	5.3	11.83
	345	6.1	13.62

	350	7.1	15.85
	355	7.9	17.63
	360	9.1	20.31
RuO_2/TiO_2-300	330	3.5	7.85
	335	4.1	9.16
	340	4.8	10.71
	345	5.5	12.28
	350	6.5	14.51
	355	7.4	16.52
	360	8.6	19.20
RuO_2/TiO_2-350	330	1.1	2.56
	335	1.4	3.10
	340	1.7	3.79
	345	2.0	4.46
	350	2.4	5.36
	355	2.9	6.47
	360	3.5	7.81

[a] Reaction conditions: Catalyst particle sizes = 0.180-0.250 mm, *V* (HCl) = 300 mL min^{-1}, WHSV (HCl) = 2933 h^{-1}, molar ratio of HCl to O_2 = 4 : 1. The reaction rates were measured after 1 h of the reaction.

Table S3 Data for calculating the Mears and Weisz-Prater criterion parameters

Parameters	Values
$\rho_{catal.}$	1141 kg m^{-3}
$R_{catal.}$	0.180-0.250 mm
$\rho_{catal.,g}$	4,260 kg m^{-3}
ε	0.65
τ[a]	3

[a] The pore tortuosity is assumed as 3 for a spherical catalyst particle.

Table S4 Evaluation of the Mears (C_M) and Weisz-Prater (C_{WP}) criterion parameters[a]

Catalyst	Temperature (°C)	C_M	C_{WP}
RuO_2/TiO_2-150	330	2.7×10^{-2}-3.8×10^{-2}	1.1×10^{-2}-1.6×10^{-2}
	335	3.2×10^{-2}-4.4×10^{-2}	1.3×10^{-2}-1.9×10^{-2}
	340	3.8×10^{-2}-5.2×10^{-2}	1.5×10^{-2}-2.2×10^{-2}
	345	4.5×10^{-2}-6.1×10^{-2}	1.8×10^{-2}-2.6×10^{-2}
	350	5.1×10^{-2}-7.1×10^{-2}	2.1×10^{-2}-3.0×10^{-2}
	355	6.0×10^{-2}-8.3×10^{-2}	2.4×10^{-2}-3.5×10^{-2}
	360	7.2×10^{-2}-9.8×10^{-2}	2.9×10^{-2}-4.2×10^{-2}
RuO_2/TiO_2-200	330	3.3×10^{-2}-4.6×10^{-2}	1.3×10^{-2}-1.9×10^{-2}
	335	3.9×10^{-2}-5.4×10^{-2}	1.6×10^{-2}-2.3×10^{-2}
	340	4.5×10^{-2}-6.2×10^{-2}	1.8×10^{-2}-2.6×10^{-2}
	345	5.3×10^{-2}-7.2×10^{-2}	2.1×10^{-2}-3.1×10^{-2}
	350	6.0×10^{-2}-8.3×10^{-2}	2.1×10^{-2}-3.5×10^{-2}
	355	7.0×10^{-2}-1.1×10^{-1}	2.8×10^{-2}-4.1×10^{-2}
	360	8.1×10^{-2}-2.1×10^{-2}	3.3×10^{-2}-4.7×10^{-2}
RuO_2/TiO_2-250	330	4.0×10^{-2}-5.6×10^{-2}	1.6×10^{-2}-2.4×10^{-2}
	335	4.6×10^{-2}-6.4×10^{-2}	1.9×10^{-2}-2.7×10^{-2}
	340	5.3×10^{-2}-7.3×10^{-2}	2.1×10^{-2}-3.1×10^{-2}
	345	6.1×10^{-2}-8.3×10^{-2}	2.5×10^{-2}-3.5×10^{-2}
	350	7.0×10^{-2}-9.6×10^{-2}	2.8×10^{-2}-4.1×10^{-2}
	355	7.8×10^{-2}-1.1×10^{-1}	3.2×10^{-2}-4.5×10^{-2}

	360	8.9×10^{-2}-1.2×10^{-1}	3.6×10^{-2}-5.2×10^{-2}
RuO_2/TiO_2-300	330	3.5×10^{-2}-4.9×10^{-2}	1.4×10^{-2}-2.1×10^{-2}
	335	4.1×10^{-2}-5.7×10^{-2}	1.7×10^{-2}-2.4×10^{-2}
	340	4.8×10^{-2}-6.6×10^{-2}	1.9×10^{-2}-2.8×10^{-2}
	345	5.5×10^{-2}-7.5×10^{-2}	2.2×10^{-2}-3.2×10^{-2}
	350	6.4×10^{-2}-8.8×10^{-2}	2.6×10^{-2}-3.8×10^{-2}
	355	7.3×10^{-2}-1.0×10^{-1}	3.0×10^{-2}-4.3×10^{-2}
	360	8.4×10^{-2}-1.2×10^{-1}	3.4×10^{-2}-4.9×10^{-2}
RuO_2/TiO_2-350	330	1.1×10^{-2}-1.5×10^{-2}	4.5×10^{-3}-6.5×10^{-3}
	335	1.4×10^{-2}-1.9×10^{-2}	5.7×10^{-3}-8.2×10^{-3}
	340	1.7×10^{-2}-2.3×10^{-2}	6.9×10^{-3}-9.9×10^{-3}
	345	2.0×10^{-2}-2.7×10^{-2}	8.1×10^{-3}-1.2×10^{-2}
	350	2.4×10^{-2}-3.3×10^{-2}	9.6×10^{-3}-1.4×10^{-2}
	355	2.9×10^{-2}-3.9×10^{-2}	1.2×10^{-2}-1.7×10^{-2}
	360	3.4×10^{-2}-4.7×10^{-2}	1.4×10^{-2}-2.0×10^{-2}

[a] Reaction conditions: Catalyst particle sizes = 0.180-0.250 mm, *V* (HCl) = 300 mL min^{-1}, WHSV (HCl) = 2933 h^{-1}, molar ratio of HCl to O_2 = 4 : 1.

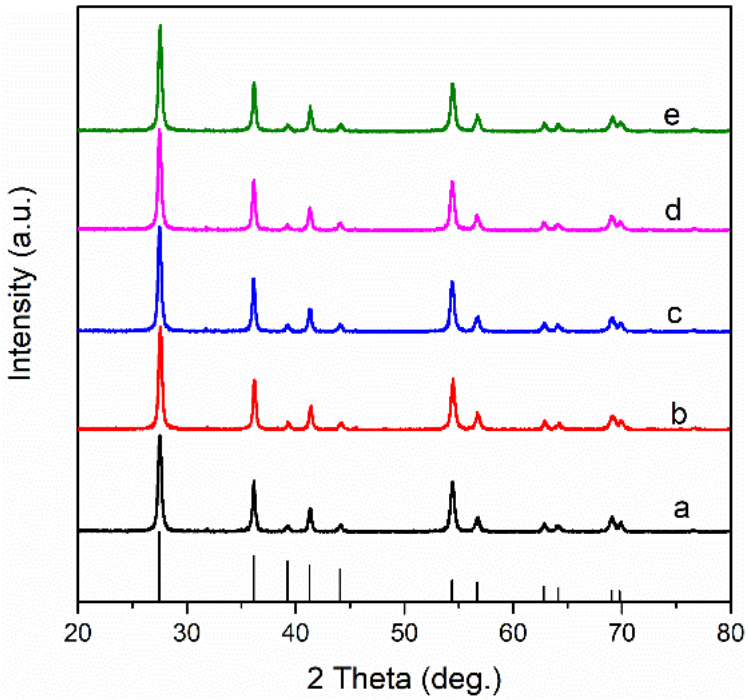

Fig. S1 Wide-angle XRD patterns of RuO_2/TiO_2-150 (a), RuO_2/TiO_2-200 (b), RuO_2/TiO_2-250 (c), RuO_2/TiO_2-300 (d), and RuO_2/TiO_2-350 (e). The standard pattern of rutile-type TiO_2 (JCPDS No. 21-1276) is shown at the bottom of the figure.

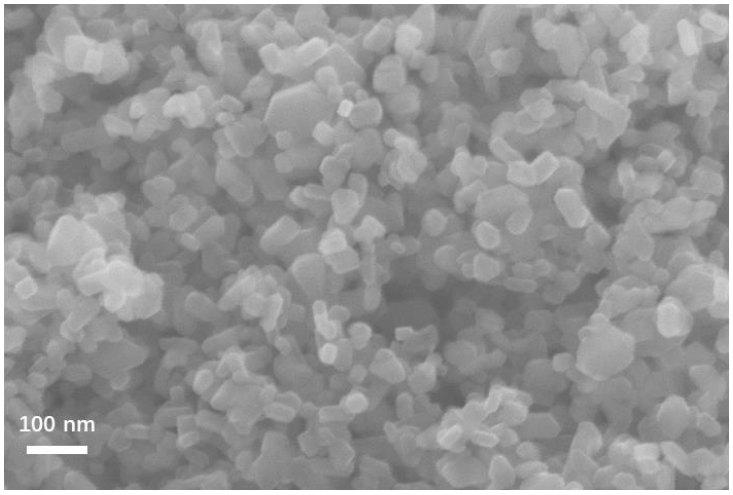

Fig. S2 SEM image of TiO_2.

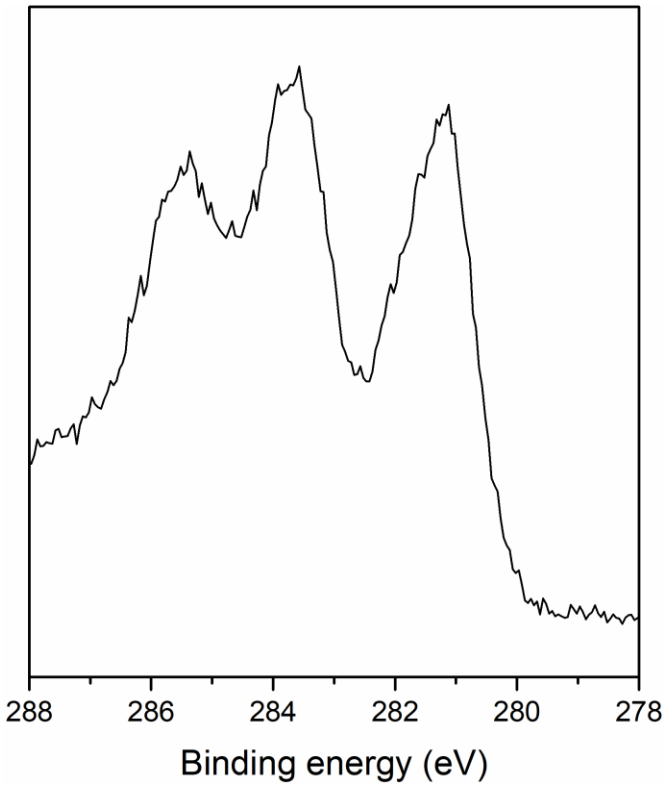

Fig. S3 Ru 3d XPS spectrum of $RuCl_3/TiO_2$.

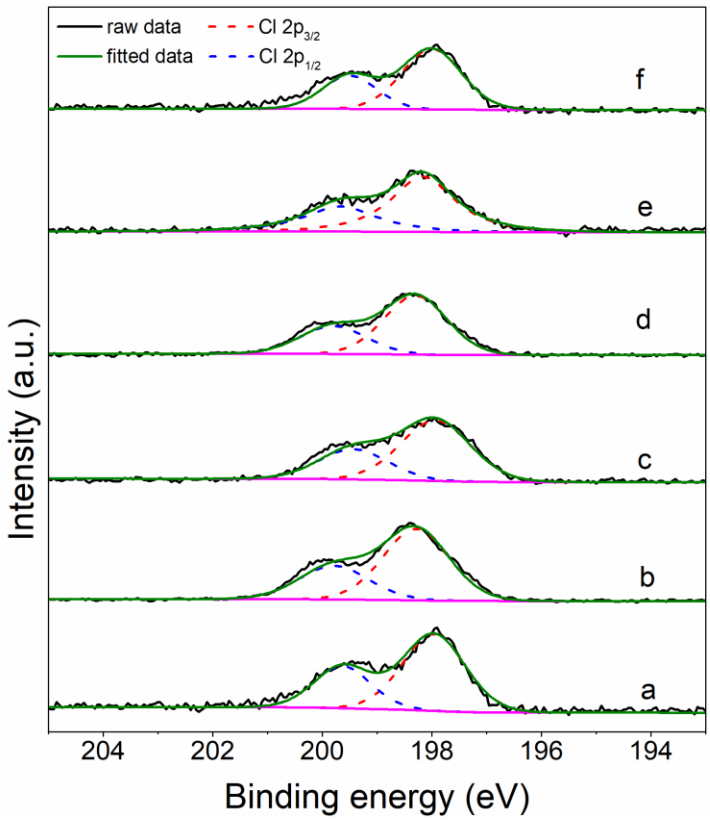

Fig. S4 Cl 2p XPS spectra of $RuCl_3/TiO_2$ (a), RuO_2/TiO_2-150 (b), RuO_2/TiO_2-200 (c), RuO_2/TiO_2-250 (d), RuO_2/TiO_2-300 (e), and RuO_2/TiO_2-350 (f).

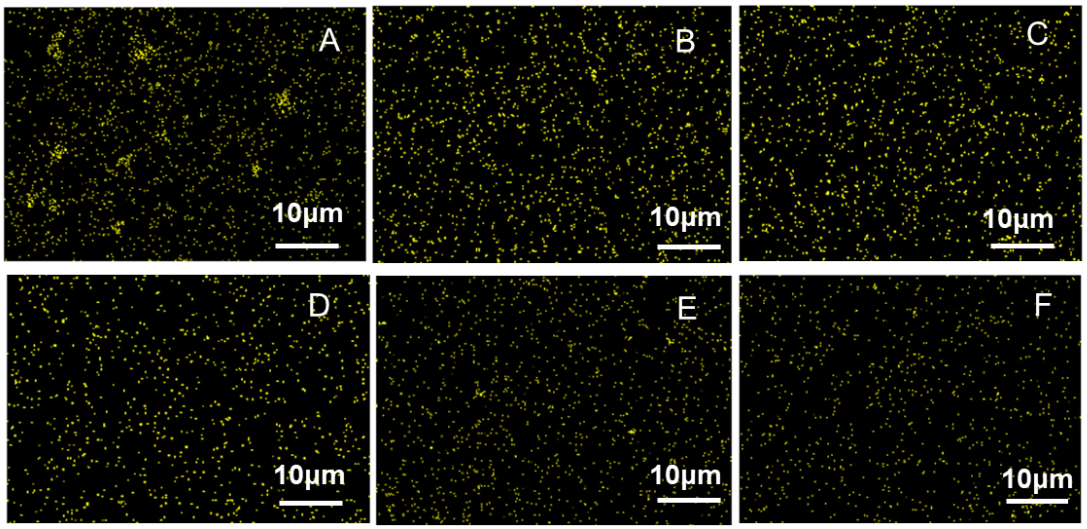

Fig. S5 EDX mapping images of Cl for $RuCl_3/TiO_2$ (A), RuO_2/TiO_2-150 (B), RuO_2/TiO_2-200 (C), RuO_2/TiO_2-250 (D), RuO_2/TiO_2-300 (E), and RuO_2/TiO_2-350 (F).

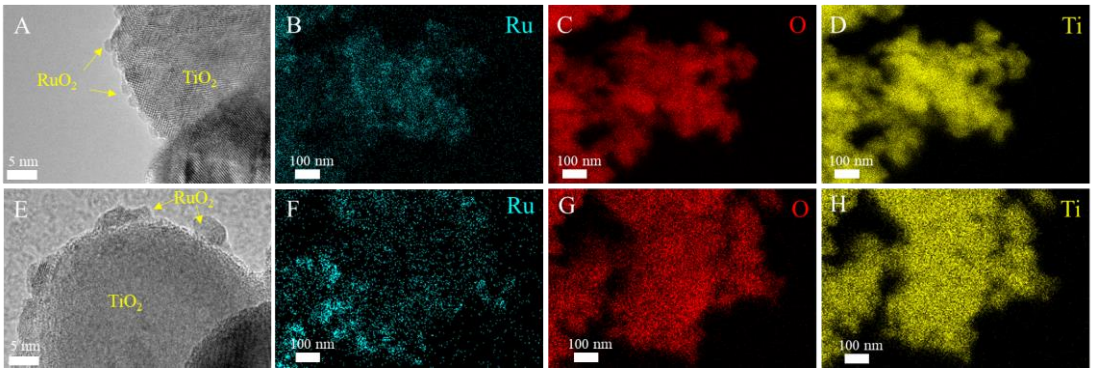

Fig. S6 TEM (A, E) and EDX mapping images of Ru (B, F), O (C, G), and Ti (D, H) of RuO_2/TiO_2-250 (A-D) and RuO_2/TiO_2-350 (E-H).

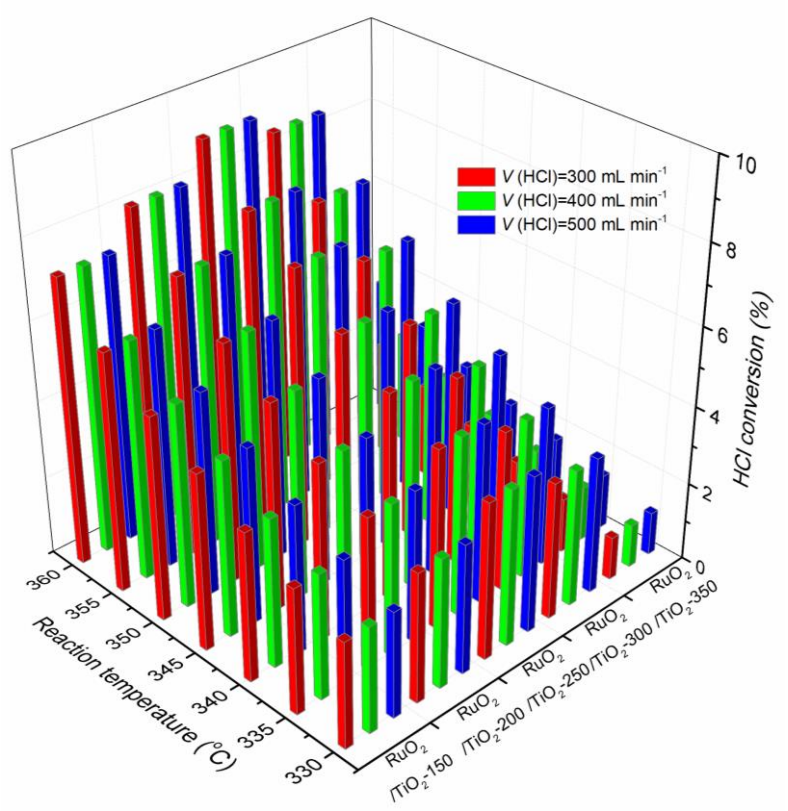

Fig. S7 Effects of HCl flow rate and reaction temperature on the catalytic activities in the oxidation of HCl with O_2 over different RuO_2/TiO_2 catalysts. Reaction conditions: catalyst particle sizes = 0.180-0.250 mm, WHSV (HCl) = 2933 h^{-1}, and molar ratio of HCl to O_2 = 4 : 1.

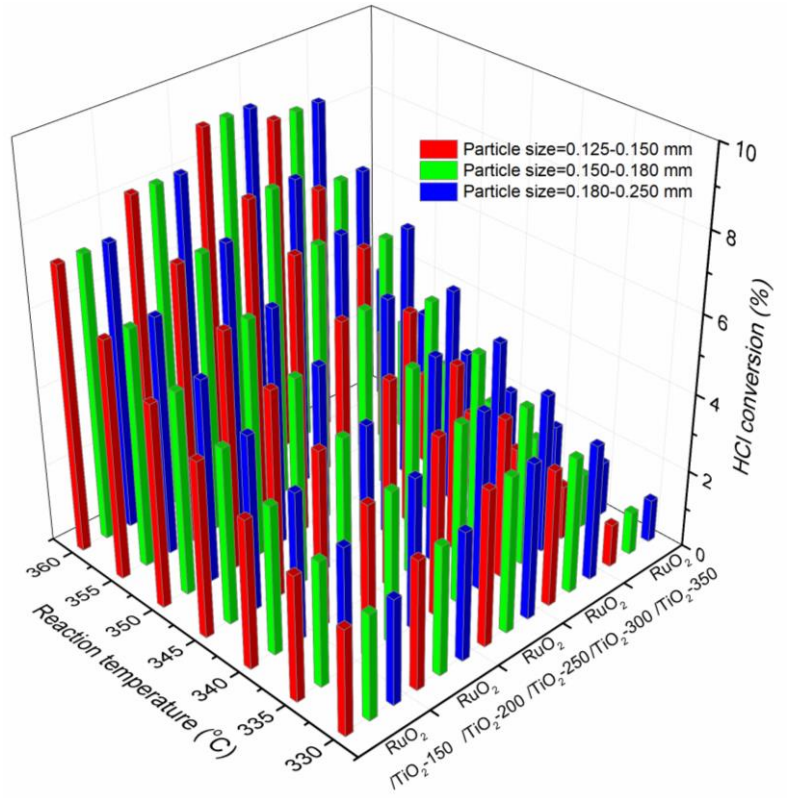

Fig. S8 Effects of catalyst particle size and reaction temperature on the catalytic activities in the oxidation of HCl with O_2 over different RuO_2/TiO_2 catalysts. Reaction conditions: WHSV (HCl) = 2933 h^{-1} and molar ratio of HCl to O_2 = 4 : 1.

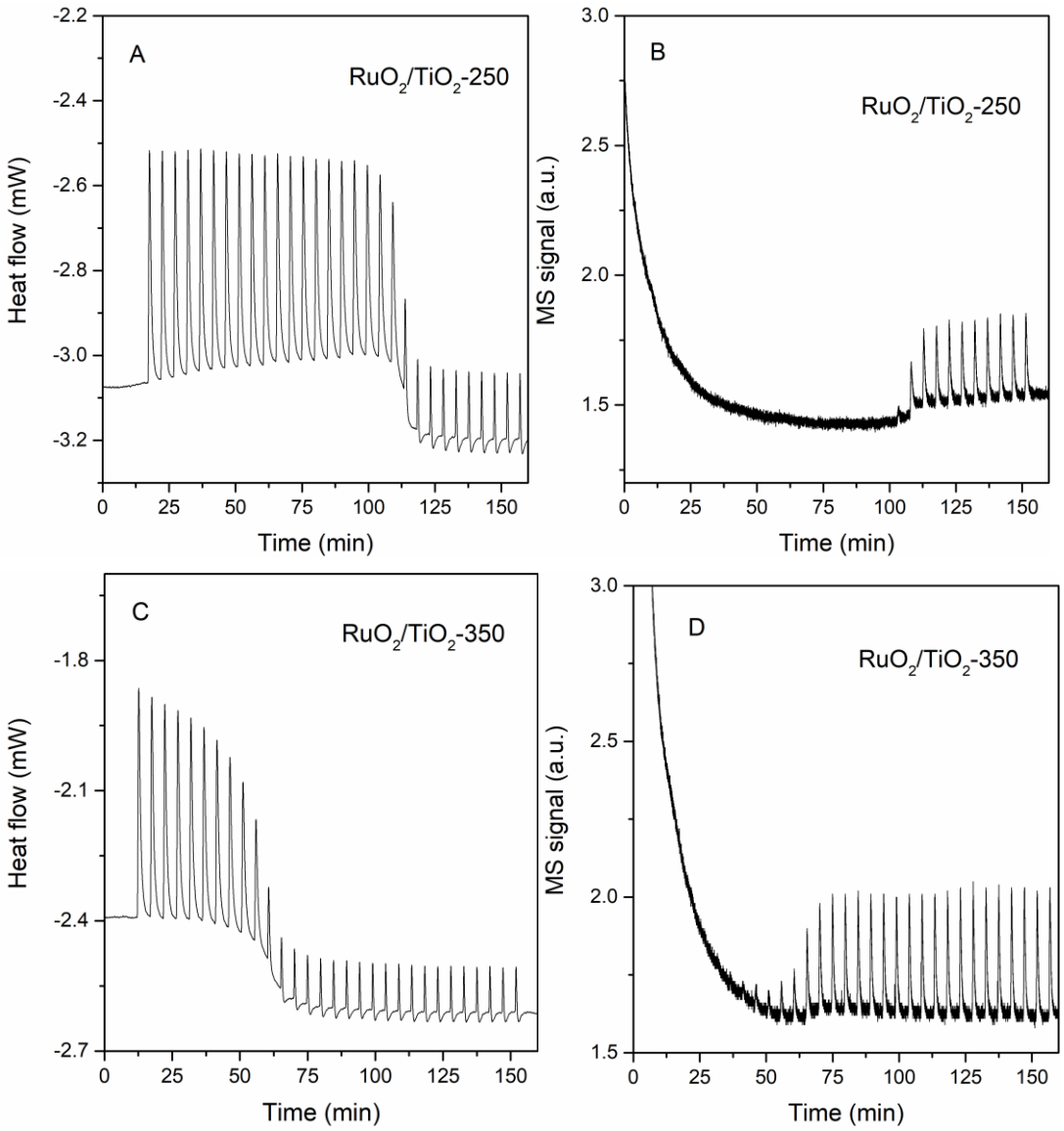

Fig. S9 Heat flow and MS signals in the microcalorimetric measurements on the pulse adsorption of O_2 on RuO_2/TiO_2-250 (A, B) and RuO_2/TiO_2-350 (C, D), respectively, as a function of time at 350 °C.

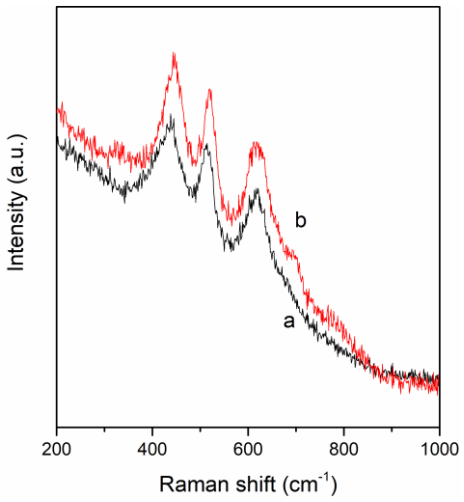

Fig. S10 Raman spectra of the fresh RuO_2/TiO_2-350 (a) and the used RuO_2/TiO_2-350 (b). The used catalyst represents the catalyst after 32 h of the reaction at 350 °C, and the reaction conditions were the same as those described in the caption of Fig. 4.

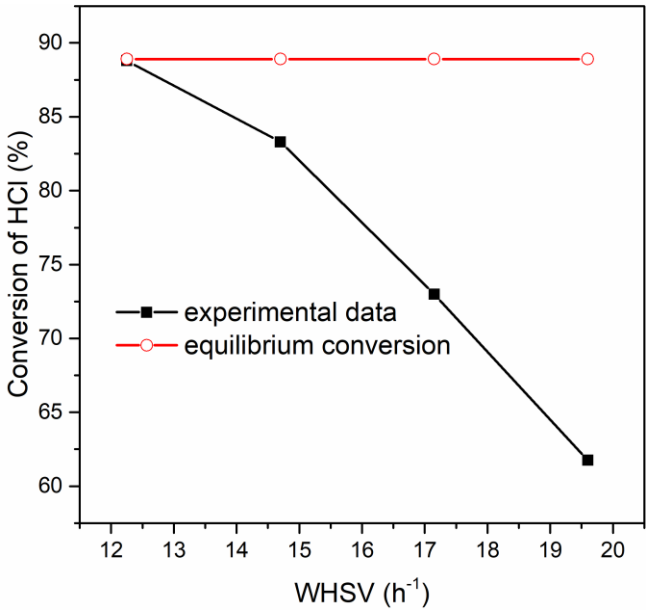

Fig. S11 Effects of WHSV on the oxidation of HCl over RuO_2/TiO_2-250. Reaction conditions: molar ratio of HCl to O_2 = 1 : 1 and reaction temperature = 350 °C.